# Ethylene-Vinyl Alcohol Copolymers Partially Modified With Benzoate Groups: Study of Their Polymorphic Behavior

**M. SÁNCHEZ-CHAVES,[1] M. FERNÁNDEZ-GARCÍA,[1] M. L. CERRADA[2]**

[1]Departamento de Química y Propiedades de Materiales Poliméricos, Instituto de Ciencia y Tecnología de Polímeros (CSIC), C/ Juan de la Cierva, 3, 28006 Madrid, Spain

[2]Departamento de Química-Física de Polímeros, Instituto de Ciencia y Tecnología de Polímeros (CSIC), C/ Juan de la Cierva, 3, 28006 Madrid, Spain

*Received 6 July 2006; revised 6 November 2006; accepted 20 November 2006*
*DOI: 10.1002/polb.21073*
*Published online in Wiley InterScience (www.interscience.wiley.com).*

**ABSTRACT:** The crystalline structure exhibited by terpolymers obtained through chemical modification with benzoyl chloride from an ethylene-vinyl alcohol copolymer with a molar fraction in vinyl alcohol of 68%, EVOH68, has been studied by either wide angle X-ray diffraction or small angle X ray scattering experiments and differential scanning calorimetry. The type of crystal lattice developed has been found to be strongly dependent on modification degree and thermal history. A highly-disordered crystalline lattice with very small crystallites has been found for the quenched specimen with the highest benzoate content while the rest of fast cooled samples crystallized into an orthorhombic lattice. On the other hand, a monoclinic crystal cell has been observed in the slowly cooled specimens with low benzoate incorporation. At the last given thermal treatment, this monoclinic lattice evolves and seems to be transformed into an orthorhombic-like crystal for the terpolymer with the highest modification ratio. ©2007 Wiley Periodicals, Inc. J Polym Sci Part B: Polym Phys 45: 1026–1036, 2007
**Keywords:** crystallinity; crystal size; crystal structures; ethylene-vinyl alcohol copolymers; monoclinic and orthorhombic lattices; polymorphism; SAXS; X-ray

## INTRODUCTION

Ethylene-vinyl alcohol copolymers (EVOHs), which find useful applications[1] as barrier resins, adhesives, compatibilizers, etc., are essentially random copolymers and typical amphiphilic materials composed of hydrophobic and hydrophilic segments, where the properties are expected to vary widely with the copolymer composition. The relationships between the chemical composition and both crystalline structure and some physical properties have been previously investigated for series of EVOH copolymers.[2–8] These copolymers are crystalline irrespective of composition, this fact being quite unusual. It was pointed out[2] long ago that crystalline properties of poly(vinyl alcohol) (PVOH) were unchanged when a small amount of ethylene was introduced by copolymerization. It was reported later[3] that both ethylene and vinyl alcohol residues were incorporated into the crystalline regions, thus forming "mixed crystals." Other investigators,[4–9] employing thermal analysis, X-ray diffraction and $^{13}$C-NMR, have argued for similar conclusions. The existence of three types of crystalline systems depending on the composition of EVOH copolymers have been proposed:[5,6] orthorhombic for 0–20 mol % vinyl alcohol (VOH),

*Correspondence to:* M. L. Cerrada (E-mail: mlcerrada@ictp.csic.es)

Journal of Polymer Science: Part B: Polymer Physics, Vol. 45, 1026–1036 (2007)

pseudohexagonal in the composition range from 20 to 60 mol % VOH, and monoclinic for compositions above 60 mol % VOH.

Both composition and cooling rate[10] have been found to determine the crystalline structure of these EVOH copolymers. Thus, for samples slowly crystallized from the melt, a monoclinic lattice has been obtained for copolymers with compositions of 71 and 68 mol % VOH (EVOH71 and EVOH68, respectively) while a pseudohexagonal lattice has been found for a copolymer with a content of 56 mol % VOH (EVOH56). The effect of the cooling rate has been also very important, since the aforementioned copolymers with the highest VOH contents, EVOH71 and EVOH68, lead to the pseudohexagonal form when samples were quenched from the melt. EVOH56 has been found to crystallize into a pseudohexagonal lattice under all the crystallization conditions studied.[10]

The introduction of chemical groups into polymers is a very useful and general method of modifying their chemical and physical characteristics.[11] Several studies have described the chemical modification of hydroxyl functions in PVOH.[12–15] EVOH copolymers with high content in the latter co-monomer could also be very useful because, on one hand, chemical modification may be used to graft numerous functions through their hydroxyl groups and on the other hand, they are less hydrophilic and more thermally stable than PVOH. These modified polymeric materials prepared from EVOH could be used for some applications other than those aforementioned, such as materials for promoting a favored and selective adsorption of biologically active molecules and proteins and for biocide release activity, among others as reported for modified PVOH.[16–18] In this sense, different studies have described the chemical modification of hydroxyl groups in EVOH copolymers.[11,19–22]

Our research is currently focused on the development of glycopolymers by lateral introduction of carbohydrates into EVOH copolymers and on the study of properties shown for these new polymeric materials compared with those exhibited by the original EVOH copolymers. To get a deep understanding, we have considered as interesting to perform a previous study about the partial chemical incorporation of benzoate groups into EVOH copolymers as a route to obtain model polymers that could explain the effect of long substituents on the crystal structure of EVOH skeleton. Therefore, this article describes changes found in the crystalline structure of an EVOH chemically modified in homogeneous phase with benzoyl chloride at distinct compositions. This comprehensive analysis has been carried out by either wide angle X-ray diffraction (WAXD) or small angle X ray scattering (SAXS) and differential scanning calorimetry (DSC).

## EXPERIMENTAL

### Materials

A commercially available random EVOH copolymer (Kuraray) was used. The nominal composition in vinyl alcohol was 68 mol %, (EVOH68). Its density is 1.190 g $cm^{-3}$ and its melt flow index 3.1 g per10 min. The polymer was dried to constant weight under vacuum in the presence of phosphorous pentoxide.

*N*-Methyl-2-pyrrolidone (NM2P) (Fluka) was purified by distillation under vacuum and then dried for a few days with a Merck 4 Å molecular sieve. Pyridine (Ferosa) was purified by a conventional method.[23] Benzoyl chloride (Ferosa) was purified by distillation under reduced pressure immediately before its use.

### Modification of EVOH68 and Molecular Characterization

EVOH68 (30 g $L^{-1}$) was dissolved in NM2P at 90 °C, using a double-wall reactor that was entirely isolated from the outside to avoid any contact with humidity. The calculated equimolecular amounts of pyridine and benzoyl chloride were added while stirring at 15 °C. The reaction was allowed to proceed for 20 h and the polymer remained soluble throughout the process. The modified copolymers were isolated by precipitation using distilled water as precipitant. All the samples were purified by reprecipitation using dimethyl sulfoxide as solvent and distilled water as precipitant. Then, they were dried to constant weight under vacuum in the presence of phosphorous pentoxide.

The modification extent was determined by means of alkaline hydrolysis at 60 °C using a standard solution of sodium hydroxide 0.1 M and titrating back the unreacted base with 0.1 M hydrochloric acid in the presence of phenolphthalein. The modification extent was also determined by $^1$H-NMR analysis in dimethyl

**Table 1.** Characteristics of EVOH Copolymers and Terpolymers

| Sample | Modification extent (mol %)[a] | $f_c^{WAXD}$ | $L$ (Å) | $l_c$ (Å) | $T_g$[b] (°C) | $T_g$[c] (°C) | $T_m$ (°C) | $\Delta H_m$ (J g$^{-1}$) | $f_c^{DSC}$ |
|---|---|---|---|---|---|---|---|---|---|
| EVOH68-Q | 0 | 0.47 | 144 | 67.7 | 46 | 58 | 182 | 88 | 0.56 |
| EVOH68Bz1-Q | 1 | 0.37 | 127 | 47.0 | 48 | 58 | 177 | 68 | 0.44 |
| EVOH68Bz3-Q | 3 | 0.32 | 123 | 39.4 | 47 | 58 | 168 | 64 | 0.41 |
| EVOH68Bz8-Q | 8 | 0.15 | 91 | 13.7 | 50 | 54 | 156 | 50 | 0.32 |
| EVOH68-S | 0 | 0.55 | 153 | 84.2 | 55 | – | 183 | 88 | 0.56 |
| EVOH68Bz1-S | 1 | 0.50 | 147 | 73.5 | 50 | – | 178 | 70 | 0.45 |
| EVOH68Bz3-S | 3 | 0.42 | 130 | 54.6 | 52 | – | 170 | 62 | 0.40 |
| EVOH68Bz8-S | 8 | 0.35 | 126 | 44.1 | 54 | – | 156 | 48 | 0.31 |

[a] Modification extent is estimated respect to the initial 68 mol % composition in vinyl alcohol.
[b] $T_g$ estimated from the first DSC heating run.
[c] $T_g$ estimated from the second DSC heating run.

sulfoxide at 80 °C using a Bruker 300 MHz spectrometer. The results found using both methods were in agreement.

The different terpolymers obtained have been labeled taking the initial name of EVOH copolymer used, EVOH68, followed by Bz as abbreviation of benzoate groups and the degree of modification. Therefore, the distinct prepared terpolymers are: EVOH68Bz1, EVOH68Bz3, and EVOH68Bz8 in order of increasing modification extent in molar percentage: 1, 3, and 8, respectively, as listed in Table 1.

### Films Preparation

Different specimens were obtained as films by compression molding in a Collin press between hot plates at a temperature 30 °C higher than their corresponding melting points at a pressure of 2 MPa for 4 min.

The copolymer EVOH68 and each one of the different terpolymers were crystallized under two different conditions: Q and S. The first treatment, Q, consisted of a fast cooling between plates cooled with water after melting in the press. The S specimens were slowly cooled from the melt, allowing the press to cool down after switching off the power. The corresponding cooling rates were, ~100 °C min$^{-1}$ for the Q samples and 2 °C min$^{-1}$ for the S ones. Thickness of such films ranged from 150 to 180 $\mu$m.

### Structural and Thermal Characterization

Thermal properties were determined with a Perkin–Elmer DSC-7 calorimeter connected to a cooling system and calibrated with different standards. The heating rate used was 10 °C min$^{-1}$. For crystallinity determinations, a value of 156.2 J g$^{-1}$ was taken as the enthalpy of fusion of a perfectly PVOH crystalline material.[24]

Wide- (WAXD) and small-angle X-ray (SAXS) patterns were recorded in the transmission mode in the beamline A2 at HASYLAB (Hamburg, Germany) employing synchrotron radiation (with $\lambda = 0.150$ nm). WAXD profiles for all of specimens were acquired during heating experiments at a running rate of 8 °C min$^{-1}$ in time frames of 15 s, that is, with a temperature resolution of 2 °C between frames. A two-dimensional position-sensitive charge-coupled device (CCD) was used at a distance of around 25 cm from the sample. It was calibrated with the different diffractions of a crystalline poly(ethylene terephthalate) (PET) sample, and it was found to cover the spacing ranging from 0.3 to 0.9 nm. The SAXS profiles were acquired for all of samples at room temperature and for EVOH68 in a dynamic experiment at a running rate of 8 °C min$^{-1}$ in time frames of 15 s. A CCD detector was also used and was located at a distance of around 265 cm from the sample. It was now calibrated with the different orders of rat-tail cornea ($L = 65$ nm), and it was found to cover a spacing interval from 5.5 to 50 nm. The diffraction profiles were normalized to the beam intensity and corrected related to an empty sample background and also for the detector's efficiency.

## RESULTS AND DISCUSSION

Figure 1 shows the diffractograms at room temperature corresponding to EVOH68 copolymer

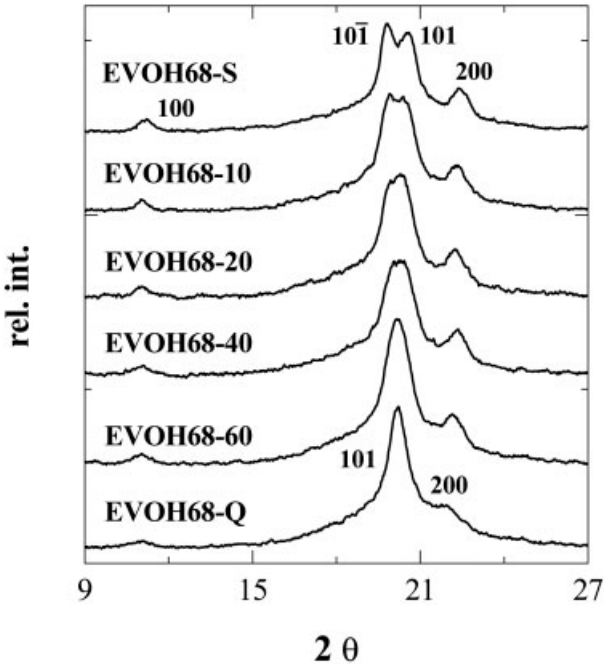


**Figure 1.** X-ray diffraction patterns at room temperature for EVOH68 prepared at different cooling rates from the melt. From rear to front: 2, 10, 20, 40, 60, and 100 °C $min^{-1}$. Profiles have been normalized to the same total intensity of the different samples.

for both thermal treatments, Q and S, together with some additional crystallization rates from the melt.[10] The diffraction pattern for the EVOH68-S (crystallized at about 2 °C $min^{-1}$) is similar to that presented by PVOH homopolymer independently of its thermal treatment, that is, corresponding to a monoclinic lattice.[6,10] On the contrary, the quenched specimen, EVOH68-Q, and that cooled down at 60 °C $min^{-1}$, lead to a pattern characteristic of a pseudohexagonal lattice (an orthorhombic one with $a$ axis equal to $c\sqrt{3}$ since the $b$ axis is the fiber axis in the EVOH copolymers; therefore, both terms will be used without distinction from now along this manuscript). On the other hand, the diffractogram of the samples cooled at 40 and 20 °C $min^{-1}$ represents an intermediate state between the two modifications, where the two main diffractions are beginning to collapse. This "transition" state is significantly dependent on VOH composition and accordingly, the monoclinic to orthorhombic transformation occurs at faster cooling rates in copolymers with VOH contents higher than EVOH68 whereas the orthorhombic form[10] is exclusively obtained under usual crystallization conditions if the content in VOH is low enough (56 mol %).

The WAXD profiles at room temperature corresponding to the different Q and S specimens here synthesized are depicted in Figure 2. At the lowest modification extent, EVOH68Bz1 sample, the two crystalline lattices, orthorhombic and monoclinic, are observed for the quenched and slowly cooled specimen, respectively, similar to the initial EVOH68. On the other hand, the intensity of the different diffractions decreases and

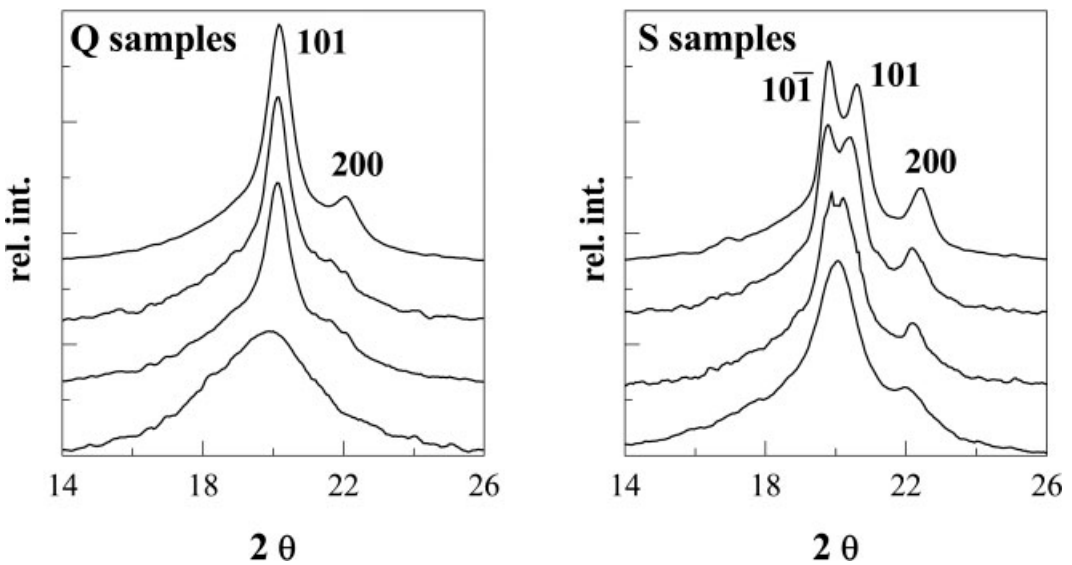


**Figure 2.** X-ray diffraction patterns at room temperature, from top to bottom, for: EVOH68, EVOH68Bz1, EVOH68Bz3 and EVOH68Bz8 quenched (left graph) and slowly cooled from the melt (right graph).

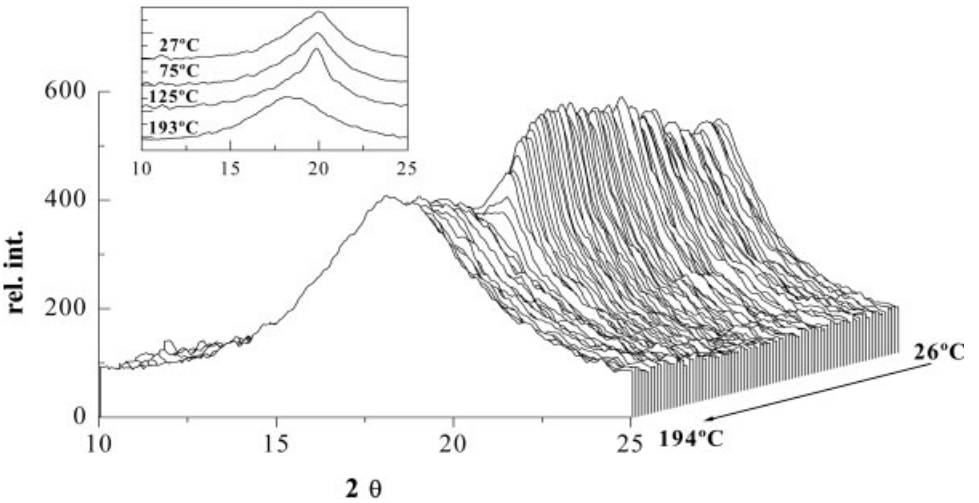


**Figure 3.** Real-time WAXD profiles, obtained with synchrotron radiation for EVOH68Bz8-Q, in a melting experiment at 8 °C $min^{-1}$. In the inset, profiles at 27, 75, 125, and 193 °C are represented.

they are broadened and shifted to slightly lower angles since, contrary to ethylene units that can be incorporated into the PVOH crystal lattice as defects, the benzoate groups are completely excluded from crystalline domains because they are much bulkier than ethylene co-monomer and, moreover, they are joint as lateral branches pendant from backbone. Consequently, benzoate incorporation implies a substantial diminishment in crystallinity and less perfect and thinner crystallites (Table 1).

The decrease in intensity diffractions, their broadness and their shift to lower angles are more evident for the terpolymer with intermediate benzoate content, EVOH68Bz3, because the average number of consecutive crystallizable units becomes smaller. Accordingly, the (200) diffraction is overlapped with the main (101) one and appears as a broad shoulder for the quenched specimen, EVOH68Bz3-Q, whereas in EVOH68Bz3-S the $(10\bar{1})$ and (101) diffractions become closer for one another analogously to the WAXD profile of EVOH68 cooled at 10 °C $min^{-1}$. This effect is even deeper in the case of EVOH68Bz8 with the highest benzoate content. When its crystallization takes place at conditions far from the equilibrium, EVOH68Bz8-Q, the development of crystallites is very limited leading to an apparently almost amorphous specimen and, on the contrary, a practically orthorhombic-like lattice is attained if crystallites perfection is allowed by a slow cooling, EVOH68Bz8-S. Accordingly, these EVOH68Bz terpolymers exhibit polymorphism with thermal treatment as initial EVOH68 copolymer and in addition, with increasing modification extent as a slow crystallization is applied.

However, a close evaluation of EVOH68Bz8-Q profile, and its just mentioned "apparently almost amorphous state," indicates that its shape is not perfectly Gaussian, suggesting a considerable, but not complete, loss of ordering (see inset in Fig. 3). The (200) reflection has disappeared and the (101) diffraction peak becomes much broader and less intense compared with that observed in the profiles of the other Q specimens. It seems that EVOH68Bz8-Q develops a much distorted lattice with crystallites very thin and imperfect. This pattern is rather similar to that reported in paraffins[25,26] and in some smectic liquid crystalline polymers.[27]

A quite analogous structure has been previously found in EVOH copolymers after stretching[28,29] identified as a strain-induce phase. In these copolymers with majority in vinyl alcohol comonomer, the deformation process takes place through necking formation up to temperatures well above their glass transition[30] and this strain-induced phase change was observed if the initial undrawn specimen exhibited either a monoclinic or orthorhombic lattice.[28] This strain-induced phase modification was characterized by the merge of the two main $(10\bar{1})$ and (101) diffractions and the disappearance of the (200) reflection at draw ratio higher than 3 in the specimens with a monoclinic cell whereas a broadening and overlapping of both (101) and (200) reflections were observed in those initial Q samples. These

features were consistent with the damage of lateral ordering just commented. A transformation from the original undrawn lattice into a disordered crystalline form of mesomorphic character was suggested in the past for uniaxially oriented polypropylene[31] and also for this type of EVOH copolymers due to their common features.[32,33]

Figure 3 shows real-time WAXD results for the EVOH68Bz8-Q specimen. The intensity of the small characteristic peak in the initial structure is kept constant within a short temperature interval (around 20 °C) and after that, intensity gradually increases: abruptly, at a first stage and in a smoother way at a second one. At temperatures higher than around 130 °C, a decrease of intensity is observed because melting process starts to take place, as represented in Figure 4(a). It has to be mentioned that a fitting program has been used to separate profiles into an amorphous component (Gaussian curve) and crystalline diffraction (Voigt function) and subsequently, to evaluate variation of crystalline peak with temperature for EVOH68Bz8-Q sample (Fig. 4). Crystallinity at room temperature for the different terpolymers analyzed, as will be discussed below, has been calculated by subtraction of the EVOH68Bz8-Q amorphous halo from the corresponding profiles. The error in the crystallinity determinations, when these are expressed as percentage in Table 1, is estimated to be ±4 units.

The inset of Figure 3 also indicates a change in diffractogram shape, additionally to the intensity variation, with increasing temperatures. Profiles shape is practically the same up to, ~85 °C (curves at 27 and 75 °C) whereas a distinguishable diffraction at around 20° appears from 85 to 130 °C due to the enhancement of ordering with temperature (see curve at 125 °C in the insert). At temperatures above, the pattern starts to broaden because melting process starts to occur. The reflection narrowness ranged from 85 to 130 °C is indicative of an increase of order within the crystalline arrangement. The derivative of profile height provides information about the phase transitions that take place within specimen. To represent the melting endotherm as a maximum, as in a DSC experiment, EVOH68Bz8-Q derivative has been normalized by −1 in Figure 4. At low temperatures, a cold crystallization of macromolecular segments that were not able to crystallize during quenching occurs within the 40–85 °C temperature range. In this temperature interval, a

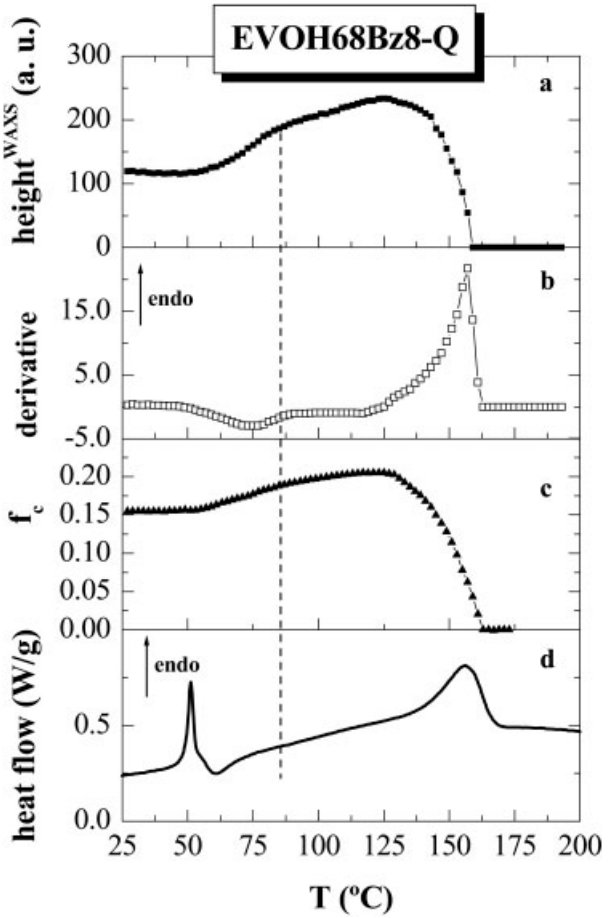


**Figure 4.** Temperature dependence of: (a) relative profile intensity; (b) its derivative; (c) $f_c^{WAXD}$ and (d) first heating DSC run, from top to bottom. Derivative has been normalized by (−1) to place the endothermic events similar to those in DSC.

slight increase in crystallinity from its initial value of about 0.15 is observed, as depicted in Figure 4. Moreover, the melting process is clearly visualized within the 125–165 °C range.

These two thermal transitions are also observed from DSC measurements during the EVOH68Bz8-Q first heating run. At low temperatures, the glass transition related to the amorphous regions occurs and is significantly overlapped with an enthalpic relaxation process (the sharp endothermic peak located at about 50 °C). This latter process is also merged with the cold crystallization in its side of high temperature. Once glass transition takes place, the mobility of the small fraction of ordered entities is enough to reorganize itself and some amorphous chains can further crystallize. Therefore, intensity of crystalline peak and, obviously, crystallinity increase. After cold crystallization is finished, intensity

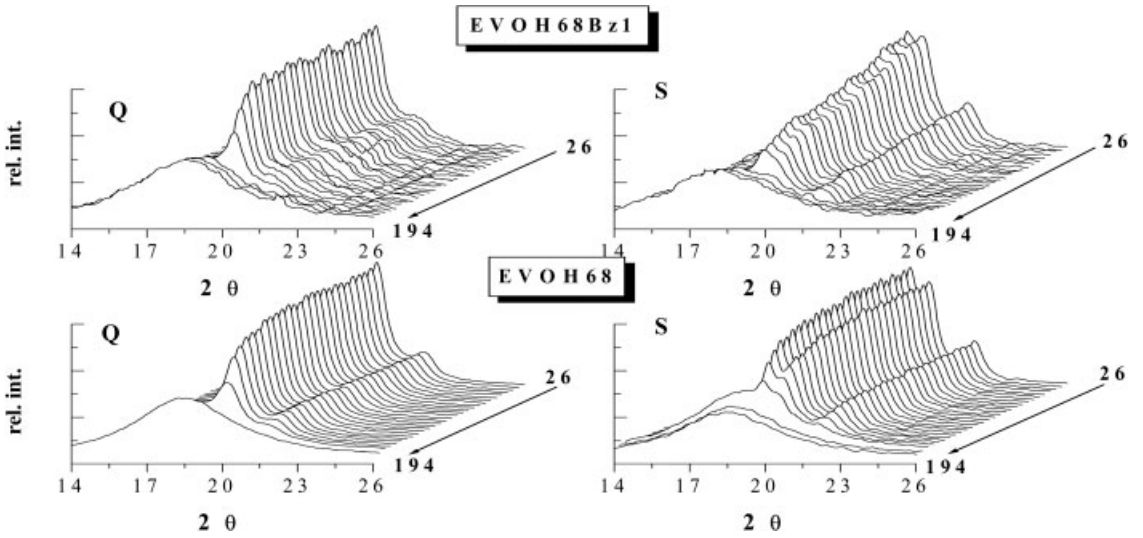


**Figure 5.** Real-time WAXD profiles for EVOH68 and EVOH68Bz1 at both thermal treatments in a melting experiment at 8 °C $min^{-1}$.

continues rising because of thickening of crystallites. Finally, these crystals melt at the highest temperature range. The agreement between location of the distinct crystalline transitions found for both WAXD and DSC experiments is very good, as seen by comparison of the different plots in Figure 4. The cold crystallization is more clearly visualized by real-time WAXD measurements because of the overlapping of this process with the enthalpic relaxation along DSC first heating running. The values of melting temperature obtained by these two techniques are in a perfect agreement.

On the other hand, the degree of crystallinity at room temperature has been directly determined for EVOH68 and its terpolymers under both thermal treatments imposed, as aforementioned, subtracting the EVOH68Bz8-Q amorphous halo, obtained by fitting of its imperfect crystalline structure, from each diffractogram. Crystallinity values thus obtained are reported in Table 1. A decrease in crystallinity is observed as benzoate content increases in the terpolymer, as previously commented from the WAXD profiles at room temperature depicted in Figure 2. In addition, slow crystallization is more amenable to crystallites development and, therefore, crystallinity degree is higher in the S sample than in that one quenched from the melt for a given specimen.

Better resolved diffractions suggest a higher ordering, and, consequently, thicker crystallites. Therefore, for a particular thermal treatment, less perfect and smaller crystals are developed in the specimens as content of benzoate groups pendant from the EVOH68 backbone is increased because the regularity disruption that they cause into the crystallizable units. This fact is confirmed by SAXS estimation at room temperature of the crystallite size in the direction normal to the lamellae, $l_c$, from the Lorentz-corrected long spacing, $L$, and the total crystallinity of the sample by assuming a simple two-phase model. The results for $l_c$ are listed in Table 1. Moreover, it can be observed that crystallites are thinner for the highest crystallization rate used since a fast cooling limits development of the crystalline entities.

Figure 5 shows real-time WAXD results for EVOH68 and EVOH68Bz1 for both thermal treatments. The melting of orthorhombic and monoclinic lattices seems to occur at a given specimen at approximately the same temperature independently of thermal history imposed during its crystallization from the melt. This feature is more clearly observed if crystalline variation with temperature is evaluated from the relative crystalline peak intensity of either the (101) reflection in the orthorhombic lattice or the two main $(10\bar{1})$ and (101) diffractions in monoclinic cell. Figure 6 represents derivatives of these intensities in those aforementioned crystalline peaks. The melting temperatures estimated from derivatives confirm again, as for EVOH68Bz8-Q, good correlation attained by comparison of DSC (Fig. 7) and WAXD data. As expected, at a given

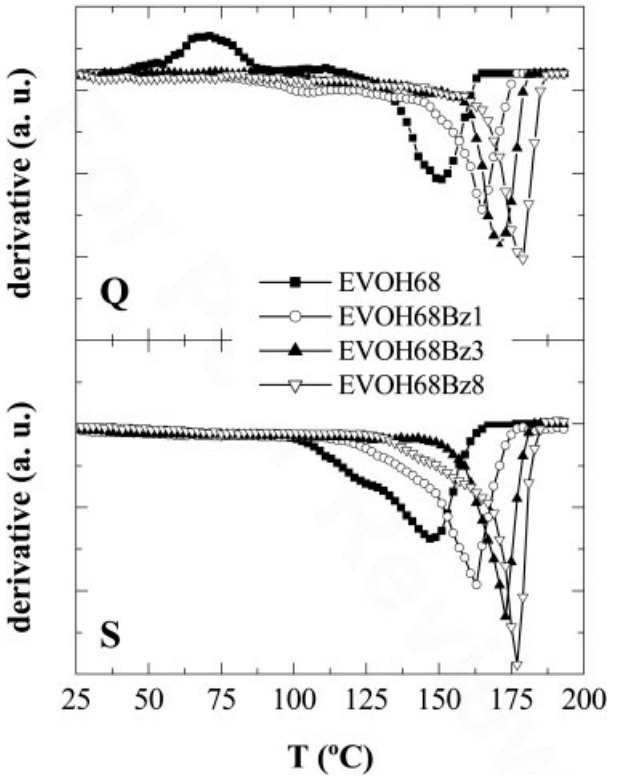


**Figure 6.** Derivative of WAXD intensity for diffraction (101) in quenched specimens (upper plot) and for $(10\bar{1})$ and (101) reflections in slowly cooled samples (lower plot).

thermal treatment, $T_m$ is depressed as benzoate groups content increases in the terpolymer due to the diminishment in crystallinity and crystallite thickness because they are very voluminous and become a hindrance for crystallization process. It is noticeable that $T_m$ decreases linearly for the terpolymers with the two lowest modification contents, EVOH68Bz1 and EVOH68Bz3 and less significantly for the EVOH68Bz8. These calorimetric results are in agreement with those recently reported by Fernández and Fernández,[22] which showed a decrease of melting points in the copolymers with an increase in the vinyl-3,5-dinitrobenzoate molar fraction. They found in their terpolymers that melting process is not longer observed above 10% of transformation.

The enthalpy values obtained at a particular specimen for both thermal histories are almost invariable similar to that constancy described for $T_m$ values (Table 1). This feature is characteristic of these EVOH copolymers[34] with high composition in vinyl alcohol independently of that they present exclusively the orthorhombic lattice or orthorhombic and monoclinic cells as function of cooling rate applied during processing. As previously commented, crystallites developed during the fast cooling are, on one hand, less perfect and thinner and, on the other hand, exhibit a broader size distribution than those promoted from a slow crystallization. Therefore, the enthalpy similarity found between the Q and S samples might be ascribed to these commented inherent characteristics in the Q crystallites that lead to continuous melt and recrystallization processes along the melting range while the thicker and perfect S crystals with a slightly narrower size distribution do undergo these melting-recrystallization-melting processes in a less extension. This assumption can be reached from Figure 8, where SAXS profiles, their invariants and their corresponding derivative results for EVOH68-Q and EVOH68-S are displayed. SAXS invariant[35] gives us idea about the macroscopic electron density fluctuations. Two different fluctuation regions are observed in EVOH68: on one hand, a clear increase of the invariant and, therefore, a kind of maximum in derivative curves

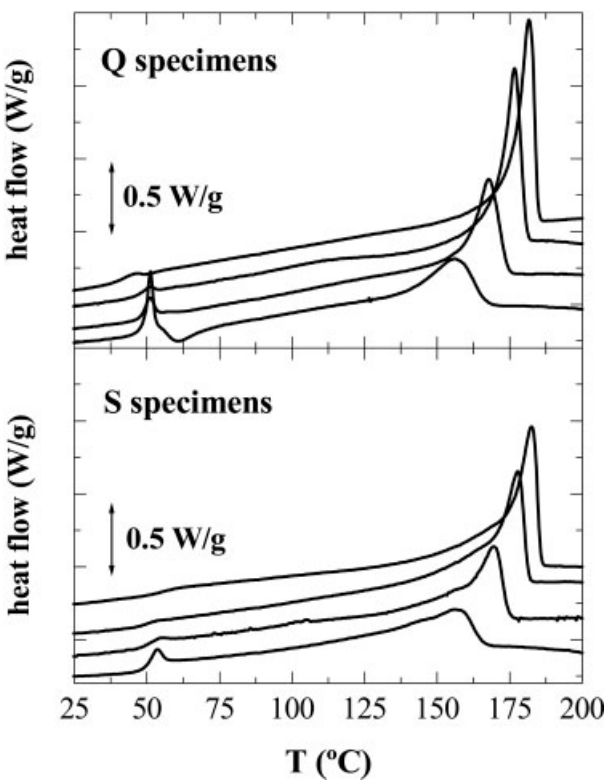


**Figure 7.** DSC first melting curves in Q and S specimens under study, upper and lower plots, respectively. From top to bottom: EVOH68, EVOH68Bz1, EVOH68Bz3, and EVOH68Bz8.

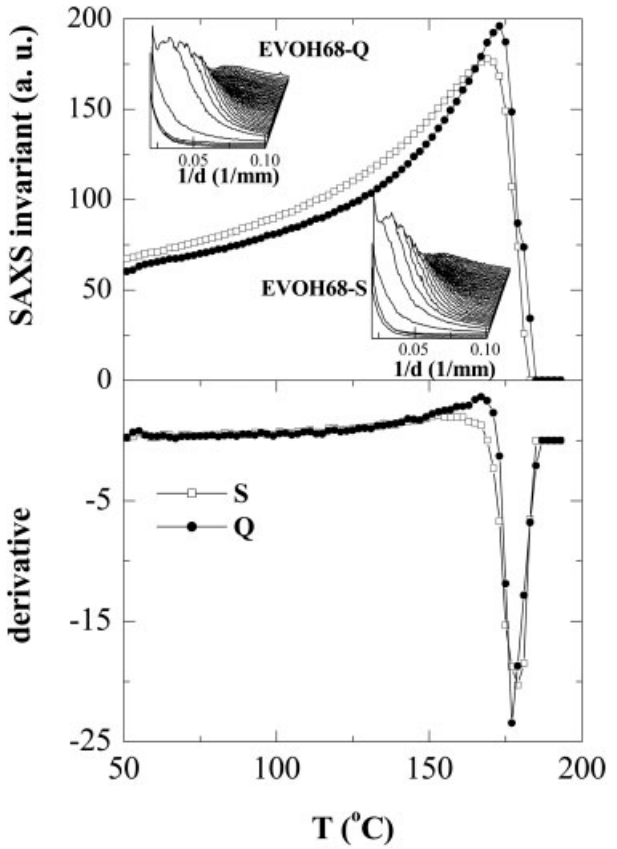


**Figure 8.** Temperature dependence of relative SAXS invariants and real-time SAXS profiles (upper plot and its insets) and SAXS invariant derivative (lower plot) in fast and slow crystallized EVOH68 specimens during the melting experiments.

(around 156 °C for S sample and 167 °C for the Q one) from room temperature to very high temperatures, indicating that recrystallization processes are involved and, on the other hand, a second fluctuation region characterized by invariant decrease associated with a narrow derivative minimum ascribed to the main melting peak. After this, the curves become flat in the molten state. This behavior found in EVOH68 is extrapolated to the other EVOH68Bz sets of terpolymers. The higher degree of recrystallization and continuous crystallites improvement found in Q specimens seems to be, accordingly, the reason of this enthalpy similarity.

Calorimetric results also evidence some characteristics of the amorphous regions. The motion restrictions caused by crystallites within the amorphous phase affect the facility of enthalpic relaxation process that occurs overlapped to glass transition.[36] This endotherm located at the top of the glass transition reflects the magnitude of this process when a sample stays below $T_g$ during some certain time. Figure 7 shows that enthalpy relaxation is inversely related to the crystallinity of the sample. The magnitude of this process is very little in EVOH68 and increases as benzoate groups composition is raised in the terpolymer because of its larger extent and its faster nonequilibrium to equilibrium evolvement. At a given specimen, it is more intense for those samples quenched from the melt. This enthalpic relaxation is completely absent during the second melting of all of the different specimens.

The overlapping of glass transition with enthalpic relaxation makes $T_g$ determination difficult during the first running of calorimetric experiments. A tentative assignment has been performed from temperature at the midpoint of the line drawn between the temperature of intersection of the initial tangent with the tangent drawn through the point of inflection of the trace and the temperature of intersection of the tangent drawn through the point of inflection with the final tangent. Results obtained are listed in Table 1 together with those estimated from the second heating run. In the Q samples, an increase of $T_g$ seems to take place while in the S specimens, a decrease followed by an increase is observed with raising modification extent. However, for the second run, a constant $T_g$ value is attained for EVOH68, EVOH68Bz1, and EVOH68Bz3 but cannot be observed for EVOH68Bz8. These opposite characteristics have a significant importance. On one hand, mobility of amorphous regions is hindered by crystallites (number and size) and by strong inter and intramolecular interactions, both of them being less as benzoate groups content increases in the terpolymer. Consequently, a decrease of $T_g$ would be expected. However, mobility of amorphous regions is, on the other hand, prevented by incorporation of benzoate groups because of their higher volume compared to that presented by nonmodified hydroxyl groups. Accordingly, an increase of $T_g$ could be predictable. The balance between these contrary effects is the key for the found behavior, the most reliable values being those calculated from the second heating run. $T_g$ is kept constant for low benzoate contents because the decreases in crystallinity and crystal size and fewer interactions are compensated by the highest volume of these groups. However, the much higher differences in

crystallites and interaction weakness cannot be balanced by the higher benzoate groups in EVOH68Bz8. Therefore, mobility in amorphous regions is enlarged and $T_g$ is shifted to lower temperatures.

## CONCLUSIONS

The partial substitution of hydroxyl groups by benzoate groups from an ethylene-vinyl alcohol copolymer points out the existence of polymorphism dependent on either thermal treatment or modification extent in these new terpolymer systems here synthesized. Therefore, for EVOH68Bz1 and EVOH68Bz3 (those terpolymers with the lower degrees of modification), the polymorphic behavior is similar to that shown in EVOH68, that is, the development of monoclinic or orthorhombic crystalline lattices for slowly or fast cooling rates, respectively. The incorporation of benzoate groups leads to a disruption of crystallizable sequences and, accordingly, crystallinity is reduced and both lattices, monoclinic and orthorhombic, become rather imperfect as modification extent is raised.

The EVOH68Bz8 shows a completely different picture for both thermal histories. A crystalline structure highly disordered is developed for the quenched specimen evolving to a more perfect arrangement by effect of temperature whereas an orthorhombic-like lattice is generated in the S sample.

Crystallinity at room temperature significantly changes with the thermal treatment at a given specimen. However, either melting temperature or enthalpy values are quite constant. These features have been associated with the higher extent of continuous melting-recrystallization-melting processes observed in the specimen EVOH68-Q by SAXS (and presumed for the rest of quenched samples) compared with that shown by slowly cooled specimen EVOH68-S due to its thicker and more perfect crystallites.

The authors are grateful to the Ministerio de Educación y Ciencia and Consejo Superior de Investigaciones Científicas (projects MAT2004-00,496 and Intramural de Frontera PIF200560F0103, respectively) for financial support. The synchrotron work (in the A2 Soft Condensed Matter beamline of Hasylab at DESY, Hamburg) was supported by the European Community-Research Infrastructure Action under the FP6 "Structuring the European Research Area" Programme (through the Integrated Infrastructure Initiative "Integrating Activity on Synchrotron and Free Electron Laser Science") (Contract RII3-CT-2004-506008). The authors thank the Hasylab personnel, especially S.S. Funari, for their collaboration.

## REFERENCES AND NOTES

1. Okaya, T.; Ikari, K. In Polyvinyl Alcohol—Developments; Finch, C. A., Ed.; Wiley: London, 1992; Chapter 8.
2. Bunn, C. W.; Peiser, H. S. Nature 1947, 159, 161.
3. Illers, K. H. Eur Polym J 1969, 5(Bratislava-Supplement), 133.
4. Bodily, D.; Wunderlich, B. J Polym Sci Part A-2: Polym Phys 1966, 4, 25.
5. Matsumoto, T.; Nakamae, K.; Ogoshi, N.; Kawasoe, M.; Oka, H. Kobunshi Kagaku 1971, 28, 610.
6. Nakamae, K.; Kameyama, M.; Matsumoto, T. Polym Eng Sci 1979, 19, 572.
7. Ramakrishnan, S. Macromolecules 1991, 24, 3753.
8. Ketels, H.; de Haan, J.; Aerdts, A.; Van der Velden, G. Polymer 1990, 31, 1420.
9. VanderHart, D. L.; Simmons, S.; Gilman, J. W. Polymer 1995, 36, 4223.
10. Cerrada, M. L.; Pérez, E.; Pereña, J. M.; Benavente, R. Macromolecules 1998, 31, 2559.
11. Bruzaud, S.; Levesque, G. Macromol Chem Phys 2000, 201, 1758.
12. Levesque, G.; Chiron, G. Ind Eng Chem Res 1987, 26, 899.
13. Arranz, F.; Bejarano, E. M.; Sánchez-Chaves, M. Macromol Chem Phys 1994, 195, 3789.
14. Baudrion, F.; Perichaud, A.; Coen, S. J Appl Polym Sci 1998, 70, 2657.
15. Gimenez, V.; Reina, J. A.; Mantecon, A.; Cadiz, V. Acta Polym 1999, 50, 187.
16. Sánchez-Chaves, M.; Arranz, F.; Cortazar, M. Polymer 1998, 39, 2751.
17. Yamaura, K.; Fukuda, M.; Tanaka, T.; Tanigami, T. J Appl Polym Sci 1999, 74, 1298.
18. Breitenbach, K.; Pistel, F.; Kissel, T. Polymer 2000, 41, 4781.
19. Marconi, W.; Piozzi, A.; Marcone, R. Eur Polym J 2001, 37, 1021.
20. Marconi, W.; Cordelli, S.; Napoli, A.; Piozzi, A. Macromol Chem Phys 1999, 200, 1191.
21. Friedmann, G.; Gandou, C.; Boiron, G.; Staveris, S.; Bouilloux, A. Eur Polym J 1998, 34, 351.
22. Fernández, M. J.; Fernández, M. D. Polymer 2005, 46, 1473.
23. Vogel, A. Textbook of Practical Organic Chemistry, 4th ed.; Longman: New York, 1978; p 277.
24. Faisant, J. B.; Aït-Kadi, A.; Bousmina, M.; Deschênes, L. Polymer 1998, 39, 533.
25. Shinohara, Y.; Kawasaki, N.; Ueno, S.; Kobayashi, I.; Nakajima, M.; Amemiya, Y. Phys Rev Lett 2005, 94, 097801.

26. Piesczek, W.; Strobl, G. R.; Malzahn, K. Acta Crystallogr Sect B 1974, 30, 1278.
27. Martínez-Gómez, A.; Bello, A.; Pérez, E. Macromol Chem Phys 2005, 206, 1731.
28. Cerrada, M. L.; Benavente, R.; Pérez, E.; Pereña, J. M. Macromol Chem Phys 2000, 201, 1858.
29. Cerrada, M. L.; Benavente, R.; Pérez, E.; Pereña, J. M. Polymer 2001, 42, 3127.
30. Cerrada, M. L.; Benavente, R.; Pereña, J. M.; Pérez, E. Polym Eng Sci 2000, 40, 1036.
31. Saraf, R. F.; Porter, R. S. Mol Cryst Liq Cryst Lett 1985, 2, 85.
32. Djezzar, K.; Penel, L.; Lefebvre, J.-M.; Séguelá, R.; Germain, Y. Polymer 1998, 39, 3945.
33. Penel, L.; Djezzar, K.; Lefebvre, J.-M.; Séguelá, R.; Fontaine, H. Polymer 1998, 39, 4279.
34. Fonseca, C.; Pereña, J. M.; Benavente, R.; Cerrada, M. L.; Bello, A.; Pérez, E. Polymer 1995, 36, 1887.
35. Ryan, J.; Stanford, J. L.; Bras, W.; Nye, T. M. W. Polymer 1997, 38, 759.
36. Struik, L. C. E. In Physical Aging in Amorphous Polymers and Other Materials. Elsevier: Amsterdam, 1978.